

A Nonlinear Navigation Observer Using IMU and Generic Position Information

Soulaimane Berkane^a, Abdelhamid Tayebi^b, Simone de Marco^c

^a *Département d'informatique et d'ingénierie, Université du Québec en Outaouais, Gatineau, Québec, Canada*

^b *Department of Electrical Engineering, Lakehead University, Thunder Bay, Ontario, Canada.*

^c *I3S, Université de Nice, Sophia-Antipolis, CNRS, France.*

Abstract

This paper deals with the problem of full state estimation for vehicles navigating in a three dimensional space. We assume that the vehicle is equipped with an Inertial Measurement Unit (IMU) providing measurements of the angular velocity, the apparent acceleration, and the body-frame Earth's magnetic field. Moreover, we consider available sensors that provide partial or full information about the position of the vehicle. Examples of such sensors are those which provide full position measurements (*e.g.*, GPS), range measurements (*e.g.*, Ultra-Wide Band (UWB) sensors), inertial bearing measurements (*e.g.*, motion capture cameras), and altitude measurements (altimeter). We propose a generic semi-globally exponentially stable nonlinear observer that estimates the position, linear velocity and attitude of the vehicle, as well as the gyro bias. We also provide a detailed observability analysis for different types of (uniform and mixed) measurements. Simulation and experimental results are provided to demonstrate the effectiveness of the proposed estimation scheme.

Key words: nonlinear observer, vehicle state estimation, inertial measurements units, position sensors.

1 Introduction

Inertial navigation systems (INS) are of great importance in many autonomous vehicles and robot platforms Titterton et al. (2004). They combine measurements from translational motion sensors (accelerometers) and rotational motion sensors (gyroscopes), to track the position, velocity and orientation of a vehicle with respect to a reference frame. Three orthogonal rate gyroscopes and three orthogonal accelerometers, measuring angular velocity and linear acceleration respectively, are typically included in an Inertial Measurement Unit (IMU) which is used, in addition to a processing unit, inside an INS system.

The use of INS alone for navigation usually leads to unreliable state estimates since measurement errors and unknown initial conditions cause the estimation error to drift over time Woodman (2007). For this reason, INS

are usually aided by position sensors such as Global Positioning Systems (GPS) which allow to correct the position estimates over time, thus, keeping the estimation errors small and bounded Grip et al. (2013). Other type of sensors that can provide range (distance) measurements to known source points can also be used to provide position information. For instance, there are some GPS receivers that provide access to the raw GPS observations (pseudo-range measurements) which are used in *tightly* coupled GPS/INS integration schemes. An advantage of the tightly coupled integration over the *loosely* coupled integration is the possibility to use few raw GPS pseudo-ranges that would otherwise be insufficient to provide a full position estimate Bryne et al. (2017); Johansen and Fossen (2016); Johansen et al. (2016). Another type of range measurement sensors that are getting popular in indoor applications is the ultra wideband (UWB) radio technology Gryte et al. (2017); Hamer and D'Andrea (2018). The idea consists in mounting a network of radio modules (anchors) at known locations along with a receiver on the vehicle. By communicating signals between the anchors and the receiver, the vehicle is able to calculate the distance (range) to the transmitting anchor in the same way a GPS receiver communicates with the satellites. The UWB-based localization technology

Email addresses: soulaimane.berkane@uqo.ca (Soulaimane Berkane), atayebi@lakeheadu.ca (Abdelhamid Tayebi), sdemarco@i3s.unice.fr (Simone de Marco).

has shown very promising accuracy in short-range applications. Ultra-short baseline (USBL) sensors are other examples of range sensors used in marine applications Batista et al. (2011, 2016). Finally, raw data from motion capture systems (*e.g.*, OptiTrack, Vicon, Xsens) can also be used as a source of position information providing inertial bearing measurements representing the projections of the relative position vectors (with respect to the fixed cameras) on the unit sphere Hamel and Samson (2017).

Although Kalman-type filters, such as Farrell (2008); Crassidis (2006); Whittaker and Crassidis (2017), are considered industry-standard solutions for inertial navigation systems, these stochastic filters are based on linearization assumptions and may fail when the initial estimation errors are large. Recently, nonlinear observers, also called deterministic estimators, have been applied in navigation systems to estimate the attitude Mahony et al. (2008); Vasconcelos et al. (2008); Berkane and Tayebi (2017c); Zlotnik et al. (2016), the attitude and the linear velocity Hua (2010); Berkane and Tayebi (2017a) and the attitude, position and linear velocity Johansen et al. (2018); Bryne et al. (2017). The advantage of the nonlinear observers is their theoretically proven guarantees (using Lyapunov methods) on the robustness and stability properties, as well as their computational simplicity compared to the stochastic filters.

In this work, we propose a semi-globally exponentially stable nonlinear observer, relying on inertial measurements and full or partial position information, for the simultaneous estimation of the position, velocity, attitude, and gyro bias of a rigid body system. The proposed observer can handle in a unified manner different type of position sensors; a feature that cannot be found in the existing observers in the literature that are usually tailored to the type of sensors used. The attitude estimates are directly obtained on the Special Orthogonal group of rotations $\mathbb{SO}(3)$, thus avoiding any singularities or ambiguities related to the use of other attitude parametrizations. A detailed study of the uniform observability property (required for the convergence of the observer) is provided. In particular, depending on the type of sensors used, we provide some weak persistency of excitation (PE) conditions guaranteeing uniform observability. Finally, note that a preliminary version of this work appeared in our conference paper Berkane and Tayebi (2019). In this extended version, we 1) provide complete proofs of the main results, 2) derive a generic observability condition on the output matrix, and conduct a detailed observability analysis with different type of position measurements, 3) experimentally validate the proposed observer on a quadrotor UAV.

The paper is organized as follows. After some preliminaries in Section 2, we formulate our estimation problem in Section 3 where we give details about the considered vehicle's model, the possible available measurements and

the technical assumptions needed for our main result. Then, in Section 4, the proposed nonlinear observer is provided and the main result is announced. In Section 5 we study the observability of the translational motion for different scenarios of position measurements. Simulation and experimental results are provided in sections 6 and 7, respectively. Finally, section 8 wraps up the paper with concluding remarks. Appendix A contains the proof of our main result.

2 Preliminaries

We denote by \mathbb{R} the set of reals and by \mathbb{N} the set of natural numbers. We denote by \mathbb{R}^n the n -dimensional Euclidean space, by \mathbb{S}^n the unit n -sphere embedded in \mathbb{R}^{n+1} and by $\mathbb{B}_\epsilon = \{x \in \mathbb{R}^3 : \|x\| \leq \epsilon\}$ the closed ball in \mathbb{R}^3 with radius ϵ . We use $\|x\|$ to denote the Euclidean norm of a vector $x \in \mathbb{R}^n$ and $\|A\|_F$ to denote the Frobenius norm of $A \in \mathbb{R}^{n \times n}$. The Special Orthogonal group of order three is denoted by $\mathbb{SO}(3) := \{A \in \mathbb{R}^{3 \times 3} : \det(A) = 1, AA^\top = A^\top A = I\}$ where I is the 3-by-3 identity matrix. The set $\mathfrak{so}(3) := \{\Omega \in \mathbb{R}^{3 \times 3} \mid \Omega^\top = -\Omega\}$ denotes the Lie algebra of $\mathbb{SO}(3)$. For $x, y \in \mathbb{R}^3$, the map $[\cdot]_\times : \mathbb{R}^3 \rightarrow \mathfrak{so}(3)$ is defined such that $[x]_\times y = x \times y$ where \times is the vector cross-product on \mathbb{R}^3 . The inverse isomorphism of the map $[\cdot]_\times$ is defined by $\text{vex} : \mathfrak{so}(3) \rightarrow \mathbb{R}^3$, such that $\text{vex}([\omega]_\times) = \omega$, for all $\omega \in \mathbb{R}^3$ and $[\text{vex}(\Omega)]_\times = \Omega$, for all $\Omega \in \mathfrak{so}(3)$. The composition map $\psi := \text{vex} \circ \mathbf{P}_{\mathfrak{so}(3)}$ extends the definition of vex to $\mathbb{R}^{3 \times 3}$, where $\mathbf{P}_{\mathfrak{so}(3)} : \mathbb{R}^{3 \times 3} \rightarrow \mathfrak{so}(3)$ is the projection map on the Lie algebra $\mathfrak{so}(3)$ such that $\mathbf{P}_{\mathfrak{so}(3)}(A) := (A - A^\top)/2$. Accordingly, for a 3-by-3 matrix $A := [a_{ij}]_{i,j=1,2,3}$, one has $\psi(A) := \text{vex}(\mathbf{P}_{\mathfrak{so}(3)}(A)) = \frac{1}{2}[a_{32} - a_{23}, a_{13} - a_{31}, a_{21} - a_{12}]$. We define $|R|_I := \frac{1}{4} \text{tr}(I - R) = \frac{1}{8} \|I - R\|_F^2 \in [0, 1]$ as the normalized Euclidean distance on $\mathbb{SO}(3)$. Given a scalar $c >$, we define the saturation function $\text{sat}_c : \mathbb{R}^n \rightarrow \mathbb{R}^n$ such that:

$$\text{sat}_c(x) := \min(1, c/\|x\|)x. \quad (1)$$

Given two scalars $c, \epsilon > 0$, we also define the smooth projection function $\mathbf{P}_c^\epsilon : \mathbb{R}^3 \times \mathbb{R}^3 \rightarrow \mathbb{R}^3$, obtained from Krstic et al. (1995), as follows:

$$\mathbf{P}_c^\epsilon(\hat{\phi}, \mu) := \begin{cases} \mu & \text{if } \|\hat{\phi}\| < c \text{ or } \hat{\phi}^\top \mu \leq 0 \\ \left(I - \theta(\hat{\phi}) \frac{\hat{\phi} \hat{\phi}^\top}{\|\hat{\phi}\|^2} \right) \mu & \text{otherwise} \end{cases} \quad (2)$$

where we let $\theta(\hat{\phi}) := \min(1, (\|\hat{\phi}\| - c)/\epsilon)$. The projection operator $\mathbf{P}_c^\epsilon(\hat{\phi}, \mu)$ is locally Lipschitz in its arguments. Moreover, provided that $\|\hat{\phi}\| \leq c$, the projection map $\mathbf{P}_c^\epsilon(\hat{\phi}, \mu)$ satisfies, along the trajectories of $\dot{\hat{\phi}} =$

$\mathbf{P}_c^\epsilon(\hat{\phi}, \mu), \|\hat{\phi}(0)\| \leq c + \epsilon$, the following properties:

$$\|\hat{\phi}(t)\| \leq c + \epsilon, \forall t \geq 0, \quad (3)$$

$$(\hat{\phi} - \phi)^\top \mathbf{P}_c^\epsilon(\hat{\phi}, \mu) \leq (\hat{\phi} - \phi)^\top \mu, \quad (4)$$

$$\|\mathbf{P}_c^\epsilon(\hat{\phi}, \mu)\| \leq \|\mu\|. \quad (5)$$

Finally, the pair $(A(\cdot), C(\cdot))$ is uniformly observable if there exist $\delta, \mu > 0$ such that, for all $t \geq 0$, the observability Gramian matrix satisfies (Bucy, 1967):

$$W(t, t + \delta) := \int_t^{t+\delta} \Phi^\top(s, t) C^\top(s) C(s) \Phi(s, t) ds \geq \mu I_n \quad (6)$$

where $\Phi(t, s)$ is the state transition matrix associated to $A(t) \in \mathbb{R}^{n \times n}$, which is defined by $\dot{\Phi}(t, s) = A(t)\Phi(t, s)$ and $\Phi(t, t) = I_n$.

3 Problem Formulation

In this paper, we consider the following dynamics of a rigid-body vehicle:

$$\dot{p} = v, \quad (7)$$

$$\dot{v} = ge_3 + Ra_B, \quad (8)$$

$$\dot{R} = R[\omega]_\times, \quad (9)$$

where $p \in \mathbb{R}^3$ is the inertial position of the vehicle's center of gravity, $v \in \mathbb{R}^3$ represents the inertial linear velocity, $R \in \mathbb{SO}(3)$ is the attitude matrix describing the orientation of a body-attached frame with respect to the inertial frame, ω is the angular velocity of the body-attached frame with respect to the inertial frame expressed in the body-attached frame, g is the norm of the acceleration due to gravity, $e_3 = [0, 0, 1]^\top$ and $a_B = R^\top a_I$ is the "apparent acceleration", capturing all non-gravitational forces applied to the vehicle, expressed in the body-attached frame.

We assume available an IMU that provides measurements of the angular velocity, the body-attached frame apparent acceleration and the body-attached frame magnetic field. These sensors are modelled as:

$$\omega^y = \omega + b_\omega \quad (10)$$

$$a_B = R^\top a_I \quad (11)$$

$$m_B = R^\top m_I \quad (12)$$

where b_ω is a constant unknown gyro bias, m_I is the constant and known earth's magnetic field and $a_I(t)$ is a time-varying unknown apparent acceleration. Note that, in practice, the above sensor measurements are usually corrupted by random noise as well. However, since in this

paper we are interested to develop a nonlinear deterministic observer, we have assumed that there is no stochastic noise in the measurements although deterministic observers are shown to have a good level of noise filtering in practice. For the rotational dynamics, the following is a general observability assumption used in the field of attitude estimation.

Assumption 1 *There exists a constant $c_0 > 0$ such that $\|m_I \times a_I(t)\| \geq c_0$ for all $t \geq 0$.*

Assumption 1 is guaranteed if the time-varying apparent acceleration $a_I(t)$ is non-vanishing and is *always* non-collinear with the constant magnetic field vector m_I . Note that $a_I(t) = 0$ corresponds to the rigid body being in a free-fall case ($\dot{v} = ge_3$) which is not likely under normal flight conditions.

We also assume in this work that we have measurements of the following position output vector:

$$y = C_p(t)p, \quad (13)$$

where $C_p(t) \in \mathbb{R}^{m \times 3}$, $m \in \mathbb{N}$, is a possibly time-varying output matrix. The measurement y can be obtained from different possible sensors, depending on the application at hand, that provide some information about the position. We will discuss some particular examples of measurements that can be written in (13) in Section 5.

The objective is to design a full navigation observer that takes the measurements (10)-(13) and outputs reliable estimates for the position p , velocity v , orientation R and gyro bias b_ω . More specifically, we want to design an exponentially convergent nonlinear observer that estimates the state of the vehicle (p, v, R, b_ω) under the above observability conditions and the following mild constraints on the trajectory of the vehicle:

Assumption 2 *There exist constants $c_1, c_2, c_3 > 0$ such that $c_1 \leq \|a_I(t)\| \leq c_2$ and $\|\dot{a}_I(t)\| \leq c_3$ for all $t \geq 0$.*

Assumption 3 *There exists constants $c_4, c_5 > 0$ such that $\|\omega(t)\| \leq c_4$ and $\|b_\omega\| \leq c_5$ for all $t \geq 0$.*

Assumptions 2 and 3 impose some realistic constraints on the systems trajectory which are needed to carry out the stability analysis.

4 Observer Design

In this section, we design our navigation observer that estimates the vehicle's state as well as the constant gyro bias. To achieve this, we first consider the extended state $x := [p^\top, v^\top, a_I^\top]^\top \in \mathbb{R}^9$ for the translational motion. In view of (7)-(8) and (13), the dynamics of x are written

as follows:

$$\dot{x} = Ax + B_1 g e_3 + B_2 \dot{a}_I \quad (14)$$

$$y = C(t)x \quad (15)$$

where the matrices A, B_1, B_2 and $C(t)$ are defined as follows:

$$A = \begin{bmatrix} 0_{3 \times 3} & I_3 & 0_{3 \times 3} \\ 0_{3 \times 3} & 0_{3 \times 3} & I_3 \\ 0_{3 \times 3} & 0_{3 \times 3} & 0_{3 \times 3} \end{bmatrix}, \quad (16)$$

$$C(t) = \begin{bmatrix} C_p(t) & 0_{m \times 3} & 0_{m \times 3} \end{bmatrix} \quad (17)$$

$$B_1 := \begin{bmatrix} 0_{3 \times 3} \\ I_3 \\ 0_{3 \times 3} \end{bmatrix}, B_2 := \begin{bmatrix} 0_{3 \times 3} \\ 0_{3 \times 3} \\ I_3 \end{bmatrix}. \quad (18)$$

The translational system (14)-(15) is a linear time-varying system with an unknown input \dot{a}_I (the jerk). The latter corresponds to the derivative of the apparent acceleration a_I which is known only in body-frame, *i.e.*, a_B . Therefore, there is a coupling between the translational dynamics (14)-(15) and the rotational dynamics (9) through the measurement equation (11) of the accelerometer. Most adhoc methods in practice assume that $a_I \approx -g e_3$ to remove this coupling between the translational and rotational dynamics. However, this assumption holds only for non-accelerated vehicles, *i.e.*, when $\dot{v} \approx 0$.

In this work, we instead design our estimation algorithm without this latter assumption. Therefore, our proposed approach will be most suitable for accelerated vehicles where the performance of adhoc approaches is low. We propose the following nonlinear navigation observer:

$$\hat{x} = \hat{z} + B_2 \hat{R} a_B, \quad (19)$$

$$\dot{\hat{z}} = A \hat{x} + B_1 g e_3 + K(t)(y - C(t)\hat{x}) + \sigma_1, \quad (20)$$

$$\dot{\hat{R}} = \hat{R}[\omega^y - \hat{b}_\omega + k_1 \sigma_2]_\times, \quad (21)$$

$$\dot{\hat{b}}_\omega = \mathbf{P}_{c_5}^{\epsilon_b}(\hat{b}_\omega, -k_2 \sigma_2), \quad (22)$$

with initial conditions $\hat{x}(0) \in \mathbb{R}^6, \hat{R}(0) \in \mathbb{SO}(3)$ and $\hat{b}_\omega(0) \in \mathbb{B}_{c_5 + \epsilon_b}$. The innovation terms $\sigma_1 \in \mathbb{R}^9$ and $\sigma_2 \in \mathbb{R}^3$ are defined as follows:

$$\sigma_1 = -k_1 B_2 [\hat{R} \sigma_2]_\times \hat{R} a_B, \quad (23)$$

$$\sigma_2 = \rho_1 (m_B \times \hat{R}^\top m_I) + \rho_2 (a_B \times \hat{R}^\top \text{sat}_{\hat{c}_2}(\hat{a}_I)), \quad (24)$$

$$\hat{a}_I = \hat{R} a_B + B_2^\top \hat{z}. \quad (25)$$

The scalars $k_1, k_2, \rho_1, \rho_2, \epsilon_b, \hat{c}_2$ are positive tuning parameters with $\hat{c}_2 > c_2$, the parameters c_2, c_5 are defined

in Assumptions 2-3, $K(t)$ is a time-varying gain matrix chosen as $K(t) = \gamma L_\gamma P(t) C(t)^\top Q(t)$, with $\gamma \geq 1$, $L_\gamma = \text{blockdiag}(I_3, \gamma I_3, \gamma^2 I_3)$ and $P(t)$ is solution to the following continuous differential Riccati-like equation:

$$\frac{1}{\gamma} \dot{P} = AP + PA^\top - PC(t)^\top Q(t) C(t) P + V(t), \quad (26)$$

where $P(0) \in \mathbb{R}^{9 \times 9}$ is positive definite, $Q(t) \in \mathbb{R}^{m \times m}$ and $V(t) \in \mathbb{R}^{9 \times 9}$ are continuous, bounded and uniformly positive definite matrices.

Before we state the stability result of the proposed observer, some remarks are in order. The proposed nonlinear observer combines the complementary filter-like attitude estimator (21)-(22), which shares a similar structure to the filter in Mahony et al. (2008), with a linear Luenberger-like observer. Since a_I is not available, we inject instead the estimate \hat{a}_I in the attitude observer while the coupling between the two observers is captured through the extra innovation term σ_1 .

Furthermore, note that if we assume $\hat{R} \equiv R$ in (19)-(20), then \hat{x} satisfies $\dot{\hat{x}} = A \hat{x} + B_1 g e_3 + B_2 \dot{a}_I + K(t)(y - C(t)\hat{x})$ which is the Luenberger observer of the translational dynamics (14)-(15). The introduction of the auxiliary state \hat{z} allows to use the information on the acceleration $a_I \equiv \hat{R} a_B$ instead of the unknown input \dot{a}_I . The additional innovation term σ_1 is used to compensate for effect of the attitude estimation error on the translational observer. Note that the innovation σ_1 vanishes as \hat{R} tends to R .

Finally, note that choosing $\gamma = 1$ in (26) yields the traditional continuous Riccati equation used in the Kalman filter where $Q^{-1}(t)$ and $V(t)$ are interpreted as the covariance matrices for the output y and the process, respectively. The introduction of the scalar γ allows for the asymptotic stability of the interconnection of the translational and rotational parts of the nonlinear observer. To state the stability result of the observer, we define the following estimation error variables:

$$\tilde{x} := x - \hat{x}, \quad (27)$$

$$\tilde{R} := R \hat{R}^\top, \quad (28)$$

$$\tilde{b}_\omega := b_\omega - \hat{b}_\omega, \quad (29)$$

$$\zeta := L_\gamma^{-1} \tilde{x}, \quad (30)$$

$$\varsigma := [|\tilde{R}|_I, \|\tilde{b}_\omega\|, \|\zeta\|]^\top. \quad (31)$$

Theorem 1 *Consider the interconnection of the dynamics (7)-(9) with the observer (19)-(25) where Assumptions 1-3 are satisfied. Assume, moreover, that the pair $(A, C(\cdot))$ is uniformly observable. Then, for each $\epsilon \in$*

$(\frac{1}{2}, 1)$ and $T > 0$ and for all initial conditions such that $\zeta(0) \in \mathbb{R}^6$, $\tilde{R}(0) \in \mathcal{U}(\epsilon) = \{\tilde{R} : |\tilde{R}(0)|_I \leq \epsilon\}$ and $\hat{b}_\omega(0) \in \mathbb{B}_{c_5 + \epsilon_b}$, there exist $k_1^* > 0$ and $\gamma^* \geq 1$ such that, for all $k_1 \geq k_1^*$ and $\gamma \geq \gamma^*$, the estimation error $\zeta(t)$ is globally uniformly bounded and

$$\|\zeta(t)\| \leq k \exp(-\lambda(t - T)) \|\zeta(T)\| \quad \forall t \geq T, \quad (32)$$

for some positive scalars k and λ .

PROOF. See Appendix A.

Theorem 1 shows that the proposed nonlinear navigation observer guarantees exponential stability of the zero estimation error provided that the initial conditions of the estimation errors lie inside a compact set which can be arbitrary enlarged by an adequate tuning of the gains. Note that the gains conditions, provided in the proof, are rather conservative and simulations have shown that the proposed navigation estimator has a large region of attraction regardless of the choice of the positive gains. Finally, the important condition on the uniform observability of the pair $(A, C(\cdot))$ will be discussed in the next section for different application scenarios.

5 Observability Analysis

A necessary condition for the result of Theorem 1 to hold is the uniform observability of the pair $(A, C(\cdot))$. This condition intuitively means that the measurement of y in (13) is enough to construct a converging translational observer (assuming perfect knowledge of the jerk \dot{a}_I) for (14)-(15). Now we derive the following important lemma.

Lemma 1 $(A, C(\cdot))$ is uniformly observable if there exist $\delta, \mu > 0$ such that for all $t \geq 0$ one has

$$\frac{1}{\delta} \int_t^{t+\delta} C_p^\top(s) C_p(s) ds \geq \mu I_3. \quad (33)$$

Moreover, if C_p is constant (A, C) is Kalman observable if and only if $\text{rank}(C_p) = 3$.

Lemma 1 provides a persistency of excitation (PE) condition on the position output matrix $C_p(t)$ whose satisfaction guarantees the required uniform observability of the pair $(A, C(\cdot))$. In the case of constant C_p the condition is equivalent to asking for the rank of the later matrix to be equal to 3. In the following subsections we will discuss this observability condition for different sets of positions sensors (range, bearing,...etc).

PROOF. [Proof of Lemma 1] First, note that A is nilpotent with index 3, i.e., $A^3 = 0$. If C_p is constant,

the rank of the observability matrix is equal to the rank of the matrix

$$\begin{bmatrix} C \\ CA \\ CA^2 \end{bmatrix} = \begin{bmatrix} C_p & 0_{m \times 3} & 0_{m \times 3} \\ 0_{m \times 3} & C_p & 0_{m \times 3} \\ 0_{m \times 3} & 0_{m \times 3} & C_p \end{bmatrix}. \quad (34)$$

It follows that the pair (A, C) is (Kalman) observable if and only if the rank of the above matrix is equal to 9, which is equivalent to $\text{rank}(C_p) = 3$. Now, let us consider the general time-varying $C_p(t)$ case. The rest of the proof is based on the result of (Hamel and Samson, 2017, Lemma 2.7). First note that

$$C^\top(t) C(t) = \begin{bmatrix} C_p^\top(t) C_p(t) & 0_{3 \times 3} & 0_{3 \times 3} \\ 0_{3 \times 3} & 0_{3 \times 3} & 0_{3 \times 3} \\ 0_{3 \times 3} & 0_{3 \times 3} & 0_{3 \times 3} \end{bmatrix} \quad (35)$$

$$= H^\top C_p^\top(t) C_p(t) H \quad (36)$$

with $H = [I_3, 0_{3 \times 3}, 0_{3 \times 3}]$. The observability Gramian matrix is the written as

$$\begin{aligned} W(t, t + \delta) &:= \int_t^{t+\delta} \Phi^\top(s, t) C^\top(s) C(s) \Phi(s, t) ds \quad (37) \\ &= \int_t^{t+\delta} \Phi^\top(s, t) H^\top C_p^\top(s) C_p(s) H \Phi(s, t) ds \quad (38) \end{aligned}$$

with $\Phi(s, t) = \exp(A(s - t))$ (since A is constant). Moreover, we have

$$\text{rank} \begin{bmatrix} H \\ HA \\ HA^2 \end{bmatrix} = \text{rank}(I_9) = 9 \quad (39)$$

which implies that the pair (A, H) is Kalman observable. Finally, all the eigenvalues of A are zero (thus real) and, therefore, in view of (33) and (Hamel and Samson, 2017, Lemma 2.7) it follows that there exist $\bar{\delta}, \bar{\mu} > 0$ such that $W(t, t + \delta) \geq \bar{\mu} I_9$ for all $t \geq 0$.

5.1 Full Position Measurement

Most GPS receivers provide position estimation when an unobstructed line of sight to four or more GPS satellites exists (*e.g.*, outdoor scenarios). In this case, the full position is assumed available and the output equation (13) is taken with $C_p(t) = I_3$. In this case, the pair (A, C) is Kalman observable since $\text{rank}(C_p) = 3$. Different algorithms such as Grip et al. (2013); Bryne et al. (2017) have developed nonlinear observers using this type of position navigation aid (loosely coupled integration). Note

that altitude determined using low-cost GPS is not generally reliable enough which can motivate the use of a pressure altimeter to determine the altitude.

5.1.1 Range Measurements

Different sensors can be used to provide range measurements. For instance, in a tightly coupled GPS/INS integration, raw GPS observations (pseudo-range measurements) are used directly in the estimation scheme to allow the use of fewer observations than actually needed to reconstruct the position. Another instance of range sensors is the UWB technology which has proved successful especially in indoor applications.

Assume that we have available n source points with known possibly time-varying locations (positions)¹, denoted as p_i . The corresponding range measurements are given by

$$d_i = \|p - p_i\|, \quad i = 1, \dots, n. \quad (40)$$

To obtain an output equation of type (13) we proceed as follows, see Hamel and Samson (2017). Let $\bar{y}_i := 0.5(d_i^2 - \|p_i\|^2)$ and define the weighted output

$$\bar{y}_0 := \sum_{i=1}^n \alpha_i \bar{y}_i \quad (41)$$

where $\alpha = [\alpha_1, \dots, \alpha_n] \in \mathbb{R}^n$ is a vector of constant real numbers such that $\sum_{i=1}^n \alpha_i = 1$. Now, we define our output vector as follows

$$y := \begin{bmatrix} \bar{y}_1 - \bar{y}_0 \\ \vdots \\ \bar{y}_n - \bar{y}_0 \end{bmatrix} = \begin{bmatrix} \bar{p}_1^\top \\ \vdots \\ \bar{p}_n^\top \end{bmatrix} p := C_p(t)p \quad (42)$$

where we have defined the following known vectors

$$\bar{p}_j := \sum_{i=1}^n \alpha_i (p_i - p_j), \quad j = 1, \dots, n. \quad (43)$$

(42) encodes the position information provided by the range measurements. If we have an additional altimeter sensor, the output of the altimeter can be written as $h = e_3^\top p$. In this case, and to include this measurement, we can add the row vector e_3^\top to the matrix $C_p(t)$ defined in (42).

¹ Although in most practical applications the anchors for range measurements are at constant locations, there is nothing preventing us from considering the case where these anchors are moving.

Lemma 2 $(A, C(\cdot))$ is uniformly observable if there exist $\delta, \mu > 0$ such that for all $t \geq 0$ one has

$$\frac{1}{\delta} \int_t^{t+\delta} \sum_{i=1}^n \bar{p}_i(s) \bar{p}_i^\top(s) ds + \alpha e_3 e_3^\top \geq \mu I_3. \quad (44)$$

where $\alpha = 1$ if the altimeter is used or $\alpha = 0$ otherwise.

PROOF. Condition (44) follows directly from Lemma 1 by noticing, in view of (42), that $C_p^\top(s)C_p(s) = \sum_{i=1}^n \bar{p}_i(s)\bar{p}_i^\top(s)$ when no altimeter is used, and $C_p^\top(s)C_p(s) = \sum_{i=1}^n \bar{p}_i(s)\bar{p}_i^\top(s) + e_3 e_3^\top$ when an altimeter is used.

Different conclusions can be drawn from the observability condition in Lemma 2. In the case where $n = 1$, one has $\bar{p}_1 = 0$ and therefore the condition is not fulfilled. When $n = 2$ and $\alpha = 0$, condition (44) is equivalent to a P.E. condition on the vector $p_1(t) - p_2(t)$. Roughly speaking, the latter condition prevents the vector $p_1(t) - p_2(t)$ from staying indefinitely in any plane. If we add an altimeter, *i.e.*, $n = 2$ and $\alpha = 1$, the condition prevents the vector $p_1(t) - p_2(t)$ from staying indefinitely in the plane containing e_3 . When $n = 3$ and $\alpha = 0$, condition (44) is not satisfied if the three anchors p_1, p_2 and p_3 are in the same plane for all times. However, when adding an altimeter, the condition is satisfied when the three anchors p_1, p_2 and p_3 are not aligned and e_3 does not belong to the plane spanned by the three anchors. Finally, when $n \geq 4$ the condition holds if at least 4 anchors are non-coplanar. The latter result is consistent with the minimum number of anchors required to geometrically (multilateration) find the position with no ambiguity from multiple range measurements (for stationary anchors). Adding an altimeter sensor relaxes the requirement of 4 non-coplanar anchors to 3 non-aligned anchors.

Note that in the case of constant anchors positions, the only two cases where the observability is guaranteed are: 1) the case of $n \geq 4$, and 2) the case of $n = 3$ and $\alpha = 1$. In these cases the matrix C_p is constant and therefore the observability condition is also necessary as stated in Lemma 1.

Besides, we would like to emphasize that the observability condition in Lemma 2 is independent from the trajectory of the vehicle and depends only on the position of the anchors. In Hamel and Samson (2017) the variable \bar{y}_0 was added, via state augmentation, to the overall state of the system and the derived observability condition was explicitly written as a PE condition on the input. This allows to design the observer even when $n = 1$ (single range measurement) under a PE condition

on the input. However the focus of Hamel and Samson (2017) was on position estimation only, whereas here we consider the full navigation problem. Handling the case of single range measurements, via state augmentation, for the full navigation problem exceeds the scope of this paper.

5.1.2 Bearing Measurements

A motion capture system consisting of a stationary array of cameras capturing the vehicle from multiple angles can be used to provide raw bearing measurements in the inertial frame. Each camera can provide a unit vector direction measurement as follows:

$$y_i = R_i^\top \frac{p - p_i}{\|p - p_i\|}, \quad i = 1, \dots, n, \quad (45)$$

where $R_i \in \mathbb{SO}(3)$ is the known orientation of the i -th camera with respect to the inertial frame, p_i is the inertial position of the i -th camera and n is the number of working cameras. Note that here we consider bearings measured in the inertial frame in contrast to Hamel and Samson (2018) for examples where bearings are measured in the body frame of reference. Following Hamel and Samson (2017), we define the following output vector:

$$y = \begin{bmatrix} \Pi(y_1)R_1^\top p_1 \\ \vdots \\ \Pi(y_n)R_n^\top p_n \end{bmatrix} = \begin{bmatrix} \Pi(y_1)R_1^\top \\ \vdots \\ \Pi(y_n)R_n^\top \end{bmatrix} p := C_p(t)p. \quad (46)$$

where $\Pi : \mathbb{R}^3 \setminus \{0\} \rightarrow \mathbb{R}^{3 \times 3}$ is the orthogonal projection map defined as

$$\Pi(z) := I - \frac{zz^\top}{\|z\|^2}. \quad (47)$$

If we have an additional altimeter sensor, the output of the altimeter can be written as $h = e_3^\top p$. In this case, and to include this measurement, we can add the row vector e_3^\top to the $C_p(t)$ matrix defined in (46). In the case of the bearing measurements discussed above and a possible use of an altimeter, we state the following lemma.

Lemma 3 ($A, C(\cdot)$) is uniformly observable if there exist $\delta, \mu > 0$ such that for all $t \geq 0$ one has

$$\frac{1}{\delta} \int_t^{t+\delta} \sum_{i=1}^n \Pi(R_i y_i(s)) ds + \alpha e_3 e_3^\top \geq \mu I_3. \quad (48)$$

where $\alpha = 1$ if the altimeter is used or $\alpha = 0$ otherwise.

PROOF. Condition (48) follows directly from Lemma 1 by noticing, in view of (46), that $C_p^\top(s)C_p(s) =$

$\sum_{i=1}^n R_i \Pi(y_i(s)) R_i^\top = \sum_{i=1}^n \Pi(R_i y_i(s))$ when no altimeter is used, and $C_p^\top(s)C_p(s) = \sum_{i=1}^n \Pi(R_i y_i(s)) + e_3 e_3^\top$ when an altimeter is used.

Depending on the number of bearing measurements available and whether or not an altimeter sensor is used, we derive the following cases that fulfill the required observability condition.

Lemma 4 Assume that the velocity v is bounded. Condition (48) is satisfied if one of the following conditions holds:

- i) There exist $i, j \in \{1, \dots, n\}$ and $\epsilon > 0$, such that for all $t^* > 0$, there exists $t > t^*$, such that $\|R_i y_i(t) \times R_j y_j(t^*)\| \geq \epsilon$.
- ii) at least three cameras are not aligned.

Moreover, if the altimeter is used, condition (48) holds if either (i) or (ii) are satisfied, or one of the following conditions holds:

- iii) There exist $i \in \{1, \dots, n\}$, $\epsilon > 0$, such that for all $t^* > 0$, there exists $t > t^*$, such that $|e_3^\top R_i y_i(t)| \geq \epsilon$.
- iv) There exist $i, j \in \{1, \dots, n\}$, such that $e_3^\top (p_i - p_j) \neq 0$.

Different conclusions can be derived from Lemma 4. First, regardless whether we use an altimeter or not, if v is bounded, uniform observability is satisfied if we use

- at least one bearing measurement y_i which is not constant for all times. In other words, this requires that the vehicle is never static nor indefinitely moving in a straight line with p_i .
- at least two bearing measurements y_i and y_j which are not aligned for all times. This means that the vehicle is not indefinitely aligned with both cameras.
- at least three non-aligned cameras, regardless of the trajectory of the vehicle.

In addition, if we use the altimeter measurement, uniform observability is satisfied if

- at least one bearing measurement y_i is available, and the vehicle is not indefinitely located at the same altitude as p_i .
- at least two cameras are not at the same altitude, regardless of the vehicle's trajectory.

Interestingly, the use of an altimeter allows to obtain uniform observability for all trajectories with only two cameras installed at different altitudes. Moreover, for planar trajectories, it is sufficient to use one camera, at

a different altitude than the altimeter, to obtain uniform observability for all trajectories.

PROOF. [Proof of Lemma 4] Let us prove the result by contradiction. Assume that (48) is not satisfied. That is to say,

$$\forall \delta, \mu > 0, \exists t \geq 0, \frac{1}{\delta} \int_t^{t+\delta} \sum_{i=1}^n \Pi(R_i y_i(s)) ds + \alpha e_3 e_3^\top < \mu I_3. \quad (49)$$

Let $\{\mu_p\}_{p \in \mathbb{N}}$ be a sequence of positive numbers converging to zero and let $\delta > 0$ be arbitrary. In view of (49), there must exist a sequence of times $\{t_p\}_{p \in \mathbb{N}}$ and a sequence of unit vectors $\{z_p\}_{p \in \mathbb{N}}$ such that

$$\forall p \in \mathbb{N}, \frac{1}{\delta} \int_{t_p}^{t_p+\delta} \sum_{i=1}^n \|\Pi(R_i y_i(s)) z_p\|^2 ds + \alpha (e_3^\top z_p)^2 < \mu_p. \quad (50)$$

Since \mathbb{S}^2 is compact, there must exist a sub-sequence of $\{z_p\}_{p \in \mathbb{N}}$ that converges to some limit unit vector $\bar{z} \in \mathbb{S}^2$. It follows that

$$\lim_{p \rightarrow \infty} \frac{1}{\delta} \int_{t_p}^{t_p+\delta} \sum_{i=1}^n \|\Pi(R_i y_i(s)) \bar{z}\|^2 ds + \alpha (e_3^\top \bar{z})^2 = 0. \quad (51)$$

This is equivalent to

$$\begin{aligned} \alpha (e_3^\top \bar{z})^2 &= 0 \\ \lim_{p \rightarrow \infty} \frac{1}{\delta} \int_{t_p}^{t_p+\delta} \|\Pi(R_i y_i(s)) \bar{z}\|^2 ds &= 0, i = 1, \dots, n. \end{aligned} \quad (52)$$

Now, since v is bounded, (53) implies that

$$\lim_{p \rightarrow \infty} \|\Pi(R_i y_i(t_p + s)) \bar{z}\|^2 = 0, \quad \forall s \in (0, \delta), i = 1, \dots \quad (54)$$

Now, since $\|\Pi(y)x\|^2 = x^\top \Pi(y)x = -x^\top [y]_\times^2 x = \|y \times x\|^2$ for all $x, y \in \mathbb{S}^2$, it follows that

$$\lim_{p \rightarrow \infty} \|R_i y_i(t_p + s) \times \bar{z}\| = 0, \quad \forall s \in (0, \delta), i = 1, \dots \quad (55)$$

This also implies that

$$\forall \zeta > 0, \exists p^*, \forall p \geq p^*, \|R_i y_i(t_p + s) \times \bar{z}\| < \zeta, \quad \forall s \in (0, \delta), i = 1, \dots \quad (56)$$

Let $s \in (0, \delta/2)$ and pick $\zeta = \epsilon/2$. Then, there exists p^* such that for all $p \geq p^*$

$$\|R_i y_i(t_p + s) \times \bar{z}\| < \epsilon/2, \quad (57)$$

$$\|R_j y_j(t_p + \delta - s) \times \bar{z}\| < \epsilon/2, \quad (58)$$

for any i, j . Now since $\|x \times y\|^2 = -y^\top [x]_\times^2 y = y^\top (I_3 - xx^\top)y = 1 - (x^\top y)^2$, for all $x, y \in \mathbb{S}^2$, and using the result in (Wang and Zhang, 1994), we obtain

$$\|x \times y\| \leq \|x \times z\| + \|z \times y\|, \quad \forall x, y, z \in \mathbb{S}^2 \quad (59)$$

Using this latter fact, inequalities (57)-(58) imply that

$$\|R_i y_i(t_p + s) \times R_j y_j(t_p + \delta - s)\| < \epsilon. \quad (60)$$

Since δ can be arbitrary large and s can be arbitrary small, this last equation contradicts item i) of the Lemma. Furthermore, note that for any $t \geq 0$ and any i, j we can write

$$\|\bar{z} \times (p_i - p_j)\|^2 = \|\bar{z} \times (p(t) - p_i)\|^2 + \|\bar{z} \times (p(t) - p_j)\|^2 - 2(\bar{z} \times (p(t) - p_i))^\top (\bar{z} \times (p(t) - p_j)) \quad (61)$$

$$= \beta_i^2(t) \|\bar{z} \times R_i y_i(t)\|^2 + \beta_j^2(t) \|\bar{z} \times R_j y_j(t)\|^2 - 2\beta_i(t)\beta_j(t) (\bar{z} \times R_i y_i(t))^\top (\bar{z} \times R_j y_j(t)) \quad (62)$$

$$\quad (63)$$

$$\quad (64)$$

where $\beta_i(t) = \|p(t) - p_i\|$ and $\beta_j(t) = \|p(t) - p_j\|$. However, $\lim_{p \rightarrow \infty} \bar{z} \times R_i y_i(t_p + s) = 0$ for $i = 1, \dots$. By selecting $t = t_p + s$ and letting p go to infinity in the above equation, it follows that $\|\bar{z} \times (p_i - p_j)\|^2 = 0$ and, thus, \bar{z} is parallel to $(p_i - p_j)$ for any i and j . If we have three source points p_i, p_j and p_k that are not aligned, it is not possible to have \bar{z} to be parallel to $(p_i - p_j)$ and $(p_i - p_k)$ simultaneously. Therefore, item ii) of the lemma holds.

If the altimeter is used, (52) implies that $e_3^\top \bar{z} = e_3^\top (p_i - p_j) = 0$ which contradicts item iv) of the lemma. Finally, in view of (54), we have $\lim_{p \rightarrow \infty} ((R_i y_i(t_p + s))^\top \bar{z})^2 = 1$ and $\lim_{p \rightarrow \infty} \Pi(R_i y_i(t_p + s)) \bar{z} = 0$. Therefore,

$$\lim_{p \rightarrow \infty} e_3^\top \Pi(R_i y_i(t_p + s)) \bar{z} \quad (65)$$

$$= e_3^\top \bar{z} - \lim_{p \rightarrow \infty} (e_3^\top R_i y_i(t_p + s)) (R_i y_i(t_p + s))^\top \bar{z} \quad (66)$$

$$= \pm \lim_{p \rightarrow \infty} (e_3^\top R_i y_i(t_p + s)) \quad (67)$$

$$= 0 \quad (68)$$

for all $s \in (0, \delta)$, where we have used the fact that $e_3^\top \bar{z} = 0$ if the altimeter is used. This contradicts item iii) of the lemma.

5.2 Mixed Range/Bearing Measurements

Finally, we consider the scenario where we have a mixed set of n_r range measurements, denoted p_i^r , and n_b bearing measurements, denoted p_i^b . Following the same procedure as in (40)-(42) and (45)-(46), it is not difficult to derive the output vector y as follows:

$$y = \begin{bmatrix} \Pi(y_1)R_1^\top p_1^b \\ \vdots \\ \Pi(y_{n_b})R_{n_b}^\top p_{n_b}^b \\ \bar{y}_1 - \bar{y}_0 \\ \vdots \\ \bar{y}_{n_r} - \bar{y}_0 \end{bmatrix} = \begin{bmatrix} \Pi(y_1)R_1^\top \\ \vdots \\ \Pi(y_{n_b})R_{n_b}^\top \\ \bar{p}_1^\top \\ \vdots \\ \bar{p}_{n_r}^\top \end{bmatrix} p := C_p(t)p. \quad (69)$$

In this case the observability condition is stated in the following lemma.

Lemma 5 ($A, C(\cdot)$) is uniformly observable if there exist $\delta, \mu > 0$ such that for all $t \geq 0$ one has

$$\frac{1}{\delta} \int_t^{t+\delta} \left(\sum_{i=1}^{n_b} \Pi(R_i y_i(s)) + \sum_{i=1}^{n_r} \bar{p}_i(s) \bar{p}_i^\top(s) \right) ds + \alpha e_3 e_3^\top \geq \mu I_3. \quad (70)$$

where $\alpha = 1$ if the altimeter is used or $\alpha = 0$ otherwise.

It is clear that several observability situations can be discussed here depending on the type of sensors used. For instance, with one bearing ($n_b = 1$), two ranges ($n_r = 2$) and an altimeter, condition (70) is not satisfied if $p(t) - p_1^b$ is indefinitely orthogonal to the plan spanned by $p_1^r - p_2^r$ and e_3 . If we have two bearings and two ranges, then similar to item iv) of Lemma 4, uniform observability is guaranteed independently of the trajectory when $(p_1^r - p_2^r)^\top (p_1^b - p_2^b) \neq 0$. It is left for the reader to check all the other possible cases.

6 Simulation Results

In this section, we simulate the nonlinear observer of Section 4 with different position sensing scenarios. In all simulations, the angular velocity applied to the vehicle is given by:

$$\omega(t) = \begin{bmatrix} \sin(0.1t + \pi) \\ 0.5 \sin(0.2t) \\ 0.1 \sin(0.3t + \pi/3) \end{bmatrix} \quad (71)$$

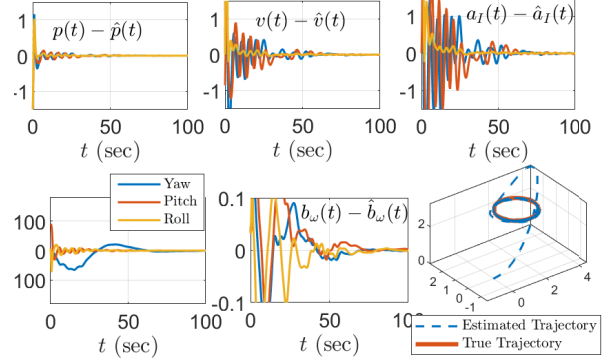


Figure 1. Estimation errors and trajectory in the case of 4 non-coplanar range measurements.

with an initial attitude $R(0) = \exp([\pi e_2]_\times / 2)$. The gyro measurements are corrupted by a constant bias of 2 (deg/sec) in each axis. The inertial earth's magnetic field is taken as $m_I = [0.033 \ 0.1 \ 0.49]^\top$ and the earth's gravity is $g = 9.81$ (m/sec²).

6.1 Range Measurements

Here we assume available four non-coplanar source points p_1, \dots, p_4 located at $p_1 = 0$ and $p_i = e_i, i = 2, 3, 4$. We consider a vehicle moving along the circular trajectory

$$p(t) = \begin{bmatrix} 1.075 \cos(\pi t/4) + 2.5 \\ 1.075 \sin(\pi t/4) + 1.5 \\ 2.2 \end{bmatrix}. \quad (72)$$

The initial conditions for the observer states are $\hat{z}(0) = \hat{b}_\omega(0) = 0, \hat{R}(0) = I_3$, and $P(0) = I_9$. The parameters of the observer are selected as $k_1 = 2, k_2 = 1, \rho_1 = 1, \rho_2 = 0.1, \epsilon_b = 0.001, c_5 = 0.06, \hat{c}_2 = 15, \gamma = 2, V(t) = I_3$ and $Q = 5I_4$. The simulation results are given in Figure 1. The proposed observer was able to recover the position, velocity, attitude and gyro bias with good precision from the IMU and range measurements.

6.2 Bearing Measurements

Here we consider inertial frame bearing measurements as described in Subsection 5.1.2. Consider a vehicle moving on following eight-shaped trajectory:

$$p(t) = \begin{bmatrix} \cos(t/2) \\ \sin(t)/4 \\ -\sqrt{3} \sin(t)/4 \end{bmatrix}. \quad (73)$$

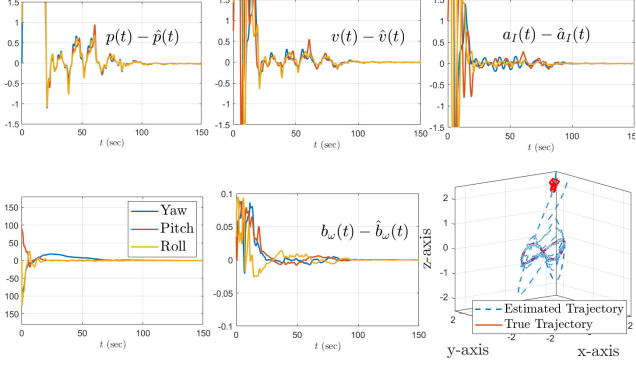


Figure 2. Estimation errors and trajectory in the case of a single bearing measurement.

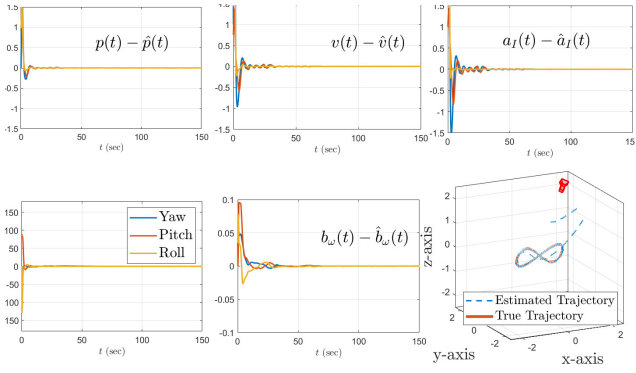


Figure 3. Estimation errors and trajectory in the case of a single bearing measurement and an altimeter sensor.

The initial conditions for the observer states are $\hat{z}(0) = [1 \ 1 \ 1 \ 1 \ 1 \ 1 \ 1 \ 1]^T$, $\hat{R}(0) = I_3$, $\hat{b}_\omega(0) = [0 \ 0 \ 0]^T$ and $P(0) = I_9$. The parameters of the observer are selected as $k_1 = 2$, $k_2 = 1$, $\rho_1 = 1$, $\rho_2 = 0.1$, $\epsilon_b = 0.001$, $c_5 = 0.06$, $\hat{c}_2 = 15$, $\gamma = 2$, $V(t) = I_3$ and $Q = I_m$. We consider two simulation scenarios. In the first scenario, we consider a single camera, located at $p_1 = [2, 2, 2]^T$ pointing towards the origin, providing a single bearing measurement. In the second scenario, we consider a single bearing measurement along with an altimeter. Figures 2 and 3 show the evolution of the different estimation errors versus time. In both scenarios, the estimation errors converge to zero. However, adding the altimeter sensor in the second scenario has considerably improved the convergence rate compared to the first simulation scenario without an altimeter.

7 Experimental results

In this section, we experimentally validate the proposed nonlinear navigation observer on a dataset recorded with a custom Quadrotor platform.

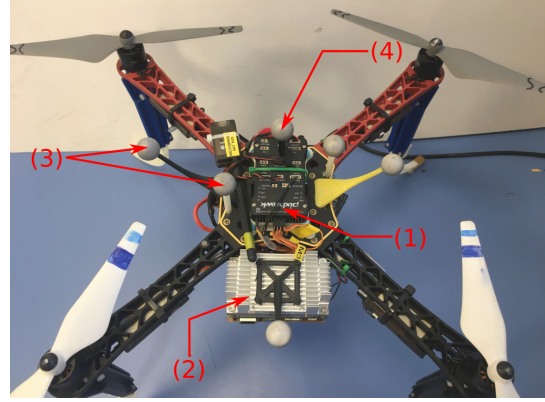


Figure 4. Quadrotor vehicle used in the experiments. (1) Pixhawk Flight Controller Unit (FCU). (2) Companion computer Nvidia Jetson TX1. (3) Optical Markers for the motion capture system (MOCAP). (4) Optical Marker used for bearings computations.

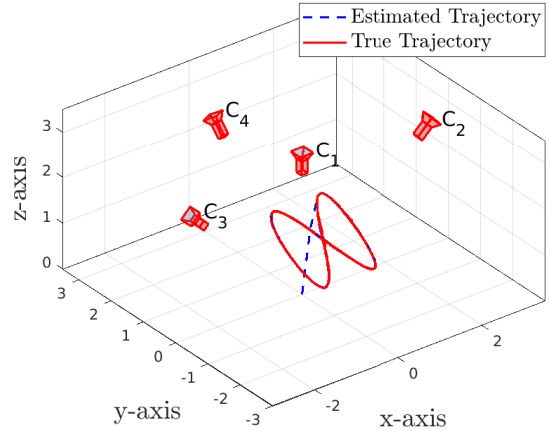


Figure 5. Position of the four cameras used for bearing measurements and 3D true trajectory vs estimated trajectory.

7.1 Experimental Setup

The vehicle (see Figure 4), based on a DJI-450 frame, is equipped with a Pixhawk flight controller unit (PX4 software) and a Nvidia Jetson TX1 as companion computer. The Pixhawk unit is equipped with a 16 bit gyroscope (L3GD20H) and 14 bit accelerometer and magnetometer sensor (LSM303D), all the sensors measurement are sent to the companion computer using mavlink/mavros protocol. A custom trajectory tracking non-linear controller based on Kai et al. (2017) has been implemented on PX4 open source flight control software.

An OptiTrack motion capture system, comprising 8 cameras, is used along with optical markers mounted on the quadrotor (see Figure 4) in order to provide full pose ground truth measurements. The good quality and high rate of the position measurement allow one to retrieve linear velocities by backwards Euler difference with rela-

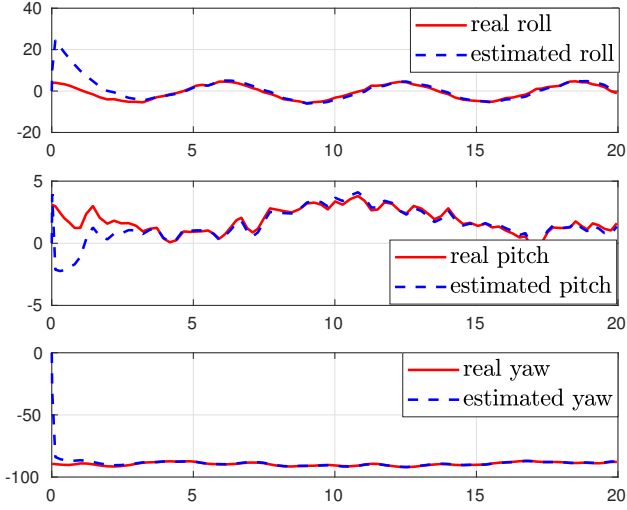


Figure 6. Time behaviour of the real and estimated roll, pitch and yaw angles.

tive low noise levels. OptiTrack Camera SDK have been used to retrieve bearing measurements of the optical marker located on the top of the Pixhawk (Figure 4 item (4)) from each camera. A ground computer, connected to the motion capture system, sends ground truth measurement and bearings to the Nvidia TX1 over WiFi.

7.2 Experiment and Results

In the experiment, the quadrotor is commanded to track the following Lemniscate trajectory (depicted in Figure 5)

$$p_{ref}(t) = \begin{bmatrix} 0.8 \cos(w_r t) \\ 0.5 + 0.8 \sin(2 * w_r t) \\ 1 + 0.8 \sin(2 * w_r t) \end{bmatrix}$$

with $w_r = 0.16\pi$, while maintaining a constant yaw angle of -90 degree. Notice that, due to the under-actuated nature of the vehicle, the roll and pitch angles can not be arbitrarily chosen and their time behaviours depend on the position control loop.

During the experiment, only four cameras have been used for bearing measurements. The inertial positions and orientations with respect to the inertial frame of the cameras (see Figure 5) are the following:

$$p_1 = \begin{bmatrix} 0 \\ 0 \\ 2.8 \end{bmatrix}, \quad p_2 = \begin{bmatrix} 2.89 \\ 0 \\ 2.57 \end{bmatrix}, \quad p_3 = \begin{bmatrix} -2.44 \\ 0 \\ 2.42 \end{bmatrix}, \quad p_4 = \begin{bmatrix} 0.08 \\ 2.65 \\ 2.37 \end{bmatrix},$$

$$q_1 = \begin{bmatrix} 0 \\ 1 \\ 0 \end{bmatrix}, \quad q_2 = \begin{bmatrix} 0.5 \\ 0 \\ -0.86 \end{bmatrix}, \quad q_3 = \begin{bmatrix} 0.45 \\ 0 \\ 0.89 \end{bmatrix}, \quad q_4 = \begin{bmatrix} 0.32 \\ 0.63 \\ -0.63 \\ 0.32 \end{bmatrix}.$$

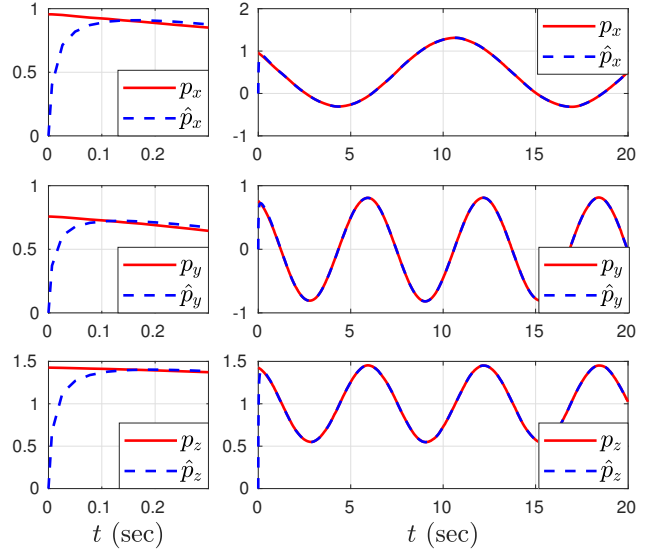


Figure 7. Time behaviour of the components of the real and estimated position (right) and zooms (left).

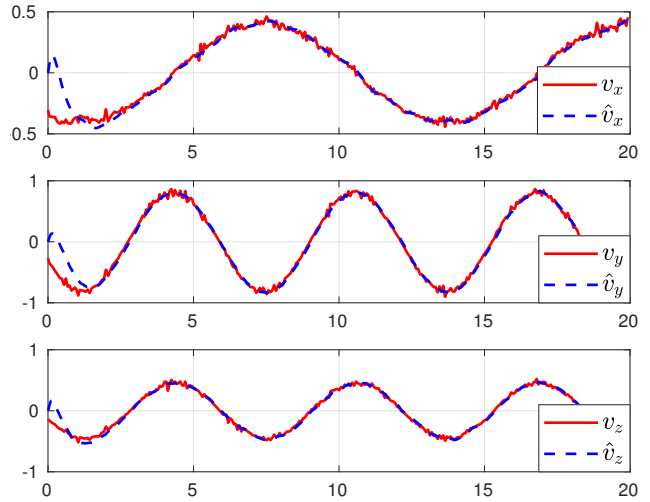


Figure 8. Time behaviour of the components of the real and estimated linear velocity.

The parameters of the observer are selected as $k_1 = 10$, $k_2 = 1$, $\rho_1 = 4$, $\rho_2 = 1.0$, $\epsilon_b = 0.001$, $c_5 = 0.3$, $\hat{c}_2 = 30$, $\gamma = 2$, $V(t) = 12I_9$ and $Q = 2I_{12}$. The initial conditions for the observer states are $\hat{z}(0) = 0_{9 \times 1}$, $\hat{R}(0) = I_3$, $\hat{b}_\omega(0) = 0_{3 \times 1}$ and $P(0) = 10I_9$.

Figure 5 shows the 3D trajectory of the vehicle versus the observer estimated trajectory, whereas Figures 6-7-8 show the time evolution of the estimated Euler RPY angles, position and velocity compared to their ground truth behaviour, respectively. Plots clearly show that the estimated attitude \hat{R} , estimated position \hat{p} and estimated velocity \hat{v} converge to the real attitude R , real position p and ground truth velocity v of the quadrotor,

respectively.

8 Conclusion

In this work, we proposed a nonlinear observer relying on IMU (accelerometer, gyroscope and magnetometer) measurements, and full/partial position information, for the simultaneous estimation of the position, velocity, orientation, and gyro bias. It employs a Riccati-like gain update which allows to possibly include the noise characteristics. The orientation estimates are obtained directly on the Special Orthogonal group of rotations. The stability of the closed-loop system is proved to be exponential with a domain of attraction that can be arbitrary enlarged. We provided a detailed observability analysis for different application scenarios involving range, bearing, or mixed range/bearing measurements, with possible use of an altimeter sensor. We show for example that the use of an altimeter relaxes the observability requirements, and increases the observer's convergence rate.

A Proof of Theorem 1

In view of (14)-(15), (19)-(21), and using the fact that $AB_2 = B_1$, one obtains

$$\begin{aligned}\dot{\hat{x}} &= \dot{x} - B_2 \hat{R} \dot{a}_B - B_2 \hat{R} \dot{a}_B - \dot{\hat{z}} \\ &= Ax + B_2(I - \tilde{R})^\top \dot{a}_I - B_2 \hat{R}[\tilde{b}_\omega + k_1 \sigma_2] \times a_B - A\hat{x} \\ &\quad - K(t)C(t)(x - \hat{x}) - \sigma_1 \\ &= (A - K(t)C(t))\tilde{x} + B_2((I - \tilde{R})^\top \dot{a}_I + \hat{R}[a_B] \times \tilde{b}_\omega) \\ &:= (A - K(t)C(t))\tilde{x} + B_2g(t, \tilde{R}, \tilde{b}_\omega).\end{aligned}\tag{A.1}$$

It follows that the auxiliary variable ζ satisfies

$$\begin{aligned}\dot{\zeta} &= L_\gamma^{-1}(A - K(t)C(t))L_\gamma\zeta + L_\gamma^{-1}B_2g(t, \tilde{R}, \tilde{b}_\omega) \\ &= \gamma(A - P(t)C(t)^\top Q(t)C(t))\zeta + \frac{1}{\gamma^2}B_2g(t, \tilde{R}, \tilde{b}_\omega),\end{aligned}\tag{A.2}$$

where we have used the following facts:

$$L_\gamma^{-1}AL_\gamma = \gamma A, \tag{A.3}$$

$$L_\gamma^{-1}B_2 = \frac{1}{\gamma^2}B_2, \tag{A.4}$$

$$C(t)L_\gamma = C(t). \tag{A.5}$$

Moreover, thanks to assumption that $(A, C(\cdot))$ is uniformly observable and the fact that $Q(t)$ and $V(t)$ are uniformly positive definite and bounded matrices, there exist (see Bucy (1972)) positive scalars β_1 and β_2 such that $\beta_1 I \leq P(t) \leq \beta_2 I$ for all $t \geq 0$. Furthermore, in view of Assumption 3 and property (3) of the projection mechanism, the bias estimation error is bounded such that $\|\tilde{b}_\omega\| \leq 2c_5 + \epsilon_b := c_b$. It follows, using Assumption

2, that

$$\begin{aligned}\|g(t, \tilde{R}, \tilde{b}_\omega)\| &\leq \sqrt{8}c_3|\tilde{R}|_I + c_2\|\tilde{b}_\omega\| \\ &\leq \sqrt{8}c_3 + c_2c_b := c_g.\end{aligned}\tag{A.6}$$

Furthermore, in view of (26), the time derivative of $P^{-1}(t)$ satisfies

$$\begin{aligned}\frac{1}{\gamma}\dot{P}^{-1} &= -P^{-1}A - A^\top P^{-1} + C^\top(t)Q(t)C(t) - P^{-1}V(t)P^{-1} \\ &= C^\top(t)Q(t)C(t) - P^{-1}V(t)P^{-1} - P^{-1}(A - PC^\top(t)Q(t)C(t)) - (A - PC^\top(t)Q(t)C(t))^\top P^{-1}.\end{aligned}\tag{A.7}$$

Now, consider the Lyapunov function candidate

$$\mathbf{V}(t, \zeta) := \frac{1}{\gamma}\zeta^\top P^{-1}(t)\zeta. \tag{A.8}$$

It follows, from (A.2), (A.6) and (A.7), that the time-derivative of $\mathbf{V}(t, \zeta)$ in (A.8) satisfies

$$\begin{aligned}\dot{\mathbf{V}}(t, \zeta) &= -\zeta^\top (C^\top(t)Q(t)C(t) + P^{-1}(t)V(t)P^{-1}(t))\zeta + \\ &\quad \frac{2}{\gamma^3}\zeta^\top P^{-1}B_2g(t, \tilde{R}, \tilde{b}_\omega) \\ &\leq -\frac{v_m}{\beta_2^2}\|\zeta\|^2 + \frac{2c_g}{\beta_1\gamma^3}\|\zeta\| \\ &\leq -\frac{v_m}{2\beta_2^2}\|\zeta\|^2, \quad \forall \|\zeta\| \geq \frac{4c_g\beta_2^2}{\gamma^3\beta_1v_m} \\ &\leq -\frac{\gamma\beta_1v_m}{2\beta_2^2}\mathbf{V}(t, \zeta), \quad \forall \|\zeta\| \geq \frac{4c_g\beta_2^2}{\gamma^3\beta_1v_m}.\end{aligned}\tag{A.9}$$

Let c_ζ and T be any two positive constant scalars. Consider the set $\Omega = \{(t, \zeta) : \mathbf{V}(t, \zeta) \leq \gamma^{-3}c_\zeta^2\beta_2^{-1}\}$. For any $(t, \zeta) \in \Omega$ one has $\|\zeta\|^2 \leq \gamma\beta_2\mathbf{V}(t, \zeta) \leq (c_\zeta\gamma^{-1})^2$. On the other hand, if $(t, \zeta) \notin \Omega$ and if we pick $\gamma \geq 2\beta_1^{-\frac{3}{4}}\beta_2^{\frac{5}{4}}c_g^{\frac{1}{2}}c_\zeta^{-\frac{1}{2}}v_m^{-\frac{1}{2}}$ then

$$\|\zeta\|^2 \geq \gamma\beta_1\mathbf{V}(\zeta) > \gamma^{-2}c_\zeta^2\beta_1\beta_2^{-1} \geq \left(\frac{4c_g\beta_2^2}{\gamma^3\beta_1v_m}\right)^2. \tag{A.10}$$

It follows in view of (A.9) that for all $(t, \zeta) \notin \Omega$ one has $\dot{\mathbf{V}}(t, \zeta) \leq -\frac{\gamma\beta_1v_m}{2\beta_2^2}\mathbf{V}(t, \zeta)$. Hence, (t, ζ) must enter Ω before the following time:

$$T^* = \frac{2\beta_2^2}{\gamma\beta_1v_m} \ln \left(\frac{\gamma^3\beta_2\mathbf{V}(0, \zeta(0))}{c_\zeta^2} \right) \tag{A.11}$$

which can be tuned arbitrary small by increasing the value of γ . The following result immediately follows:

$$\forall c_\zeta, T > 0, \forall \zeta(0), \exists \gamma_1 \geq 1 \text{ s.t. } \gamma \geq \gamma_1 \Rightarrow \|\zeta(t)\| \leq \gamma^{-1} c_\zeta, \forall t \geq T. \quad (\text{A.12})$$

Now we show that the gains can be tuned to guarantee forward invariance of the set $\mathcal{U}(\epsilon)$. Let $\epsilon \in (\frac{1}{2}, 1)$ and let the initial conditions be such that $\tilde{R}(0) \in \mathcal{U}(\epsilon)$. The time derivative of $|\tilde{R}|_I^2$, in view of (9) and (21) and making use of (Berkane et al., 2017, Lemma 2), satisfies

$$\begin{aligned} \frac{d}{dt} |\tilde{R}|_I^2 &= -\frac{1}{4} \text{tr}(\tilde{R}[-\hat{R}(\tilde{b}_\omega + k_1 \sigma_2)]_\times) \\ &= -\frac{1}{4} \text{tr}(\mathbf{P}_{\text{so}(3)}(\tilde{R})[-\hat{R}(\tilde{b}_\omega + k_1 \sigma_2)]_\times) \\ &= -\frac{1}{2} \psi(\tilde{R})^\top \hat{R}(\tilde{b}_\omega + k_1 \sigma_2) \\ &\leq \|\tilde{b}_\omega\| + k_1 \|\sigma_2\| \\ &\leq c_b + k_1(\rho_1 \|m_I\|^2 + \rho_2 c_2 \hat{c}_2) := c_R. \end{aligned}$$

Let us define $t_R := (\epsilon^2 - |\tilde{R}(0)|_I^2)/c_R$. Hence, for all $0 \leq t \leq t_R$, one has $\tilde{R}(t) \in \mathcal{U}(\epsilon)$. Pick $0 < T \leq t_R$ and $c_\zeta := \min(\bar{c}_\zeta/k_1, \hat{c}_2 - c_2)$ for some arbitrary $\bar{c}_\zeta > 0$. By (A.12) there exists $\gamma^* \geq 1$ such that if one chooses $\gamma \geq \gamma^*$ then $\|\zeta(t)\| \leq \gamma^{-1} c_\zeta$ for all $t \geq T$. In this case, one has

$$\|\hat{a}_I\| = \|a_I - \hat{a}_I - a_I\| = \|B_2^\top L_\gamma \zeta - a_I\| \leq \gamma \|\zeta\| + c_2 \leq c_\zeta + c_2 \leq \hat{c}_2. \quad (\text{A.13})$$

Consequently, for all $t \geq T$, one has $\text{sat}_{\hat{c}_2}(\hat{a}_I(t)) = a_I(t)$. It follows that the innovation term σ_2 in (24)-(25) is written as follows:

$$\begin{aligned} \sigma_2 &= \rho_1(m_B \times \hat{R}^\top m_I) + \rho_2(a_B \times \hat{R}^\top \hat{a}_I) \\ &= \rho_1(m_B \times \hat{R}^\top m_I) + \rho_2(a_B \times \hat{R}^\top a_I) + \\ &\quad \rho_2(a_B \times \hat{R}^\top (\hat{a}_I - a_I)) \\ &= 2\hat{R}^\top \psi(M\tilde{R}) - \rho_2(a_B \times \hat{R}^\top B^\top L_\gamma \zeta), \end{aligned} \quad (\text{A.14})$$

where we defined $M := \rho_1 m_I m_I^\top + \rho_2 a_I a_I^\top$ and used (Berkane and Tayebi, 2017b, Proposition 3) to derive the last equation. Note that M is positive semidefinite and has rank equals 2 (by Assumption 1). It follows that

$$\begin{aligned} \frac{d}{dt} |\tilde{R}|_I^2 &= -k_1 \psi(\tilde{R})^\top \psi(M\tilde{R}) - \frac{1}{2} \psi(\tilde{R})^\top (\hat{R} \tilde{b}_\omega - \\ &\quad k_1 \rho_2 (\hat{R} a_B) \times B^\top L_\gamma \zeta) \\ &\leq -4k_1 \lambda_{\min}^{\mathbf{E}(M)} |\tilde{R}|_I^2 (1 - |\tilde{R}|_I^2) + |\tilde{R}|_I \|\tilde{b}_\omega\| + \\ &\quad + \gamma k_1 \rho_2 c_2 |\tilde{R}|_I \|\zeta\| \\ &\leq -4k_1 \lambda_{\min}^{\mathbf{E}(M)} |\tilde{R}(t)|_I^2 (1 - |\tilde{R}(t)|_I^2) + c_b + \rho_2 c_2 \bar{c}_\zeta \end{aligned} \quad (\text{A.15})$$

where inequalities from (Berkane et al., 2017, Lemma 2) have been used with $\mathbf{E}(M) := \frac{1}{2}(\text{tr}(M) - M^\top)$ for any M . Note that the matrix $\mathbf{E}(M)$ is positive definite in view of Assumption 1. Now assume that $|\tilde{R}(t)|_I = \epsilon$ and $k_1 > (c_b + \rho_2 c_2 \bar{c}_\zeta)/(4\lambda_{\min}^{\mathbf{E}(M)} \epsilon^2 (1 - \epsilon^2))$ then, for all $t \geq T$, one has

$$\frac{d}{dt} |\tilde{R}(t)|_I^2 \leq -4k_1 \lambda_{\min}^{\mathbf{E}(M)} \epsilon^2 (1 - \epsilon^2) + c_b + \rho_2 c_2 \bar{c}_\zeta < 0.$$

This implies that $|\tilde{R}(t)|_I$ is strictly decreasing whenever $|\tilde{R}(t)|_I = \epsilon$. It follows from the continuity of the solutions that $\tilde{R}(t)$ will not leave the ball $\mathcal{U}(\epsilon)$ for all $t \geq T$. Recall also that $|\tilde{R}(t)|_I \leq \epsilon$ for all $t \leq T$ (since $T \leq t_R$). This implies that the set $\mathcal{U}(\epsilon)$ is forward invariant. Now, let us show exponential convergence. Consider the following Lyapunov function candidate:

$$\mathbf{W}(\zeta, \tilde{R}, \hat{R}, \tilde{b}_\omega) := |\tilde{R}|_I^2 + \frac{\mu_1 k_1}{2k_2} \tilde{b}_\omega^\top \tilde{b}_\omega + \mu_1 \tilde{b}_\omega^\top \hat{R}^\top \psi(\tilde{R}) + \gamma^3 \mathbf{V}(t, \zeta), \quad (\text{A.16})$$

where μ_1 is some positive constant scalar and $\mathbf{V}(t, \zeta)$ is defined in (A.8). Using the fact that $\|\psi(\tilde{R})\| \leq 2|\tilde{R}|_I$, it can be verified that \mathbf{W} satisfies the quadratic inequality $\zeta^\top P_1 \zeta \leq \mathbf{W} \leq \zeta^\top P_2 \zeta$ where the matrices P_1 and P_2 are given by

$$P_1 = \begin{bmatrix} 1 & -\mu_1 & 0 \\ -\mu_1 & \frac{\mu_1 k_1}{2k_2} & 0 \\ 0 & 0 & \frac{\gamma^2}{\beta_2} \end{bmatrix}, P_2 = \begin{bmatrix} 1 & \mu_1 & 0 \\ \mu_1 & \frac{\mu_1 k_1}{2k_2} & 0 \\ 0 & 0 & \frac{\gamma^2}{\beta_1} \end{bmatrix}.$$

Let us compute the time derivative of the cross term $\dot{\mathfrak{X}} := \tilde{b}_\omega^\top \hat{R}^\top \psi(\tilde{R})$. First, one has

$$\begin{aligned} \dot{\mathfrak{X}} &= \tilde{b}_\omega^\top \hat{R}^\top \mathbf{E}(\tilde{R}) \left(-\hat{R} \tilde{b}_\omega - k_1 \hat{R} \sigma_2 \right) - \\ &\quad \tilde{b}_\omega^\top [\omega + \tilde{b}_\omega + k_1 \sigma_2]_\times \hat{R}^\top \psi(\tilde{R}) + \\ &\quad \mathbf{P}_{c_5}^{\epsilon_b}(\hat{b}_\omega, k_2 \sigma_2)^\top \hat{R}^\top \psi(\tilde{R}). \end{aligned}$$

In addition, using (Berkane et al., 2017, (31), Lemma 2), one has the following bound

$$\begin{aligned} -\tilde{b}_\omega^\top \hat{R}^\top \mathbf{E}(\tilde{R}) \hat{R} \tilde{b}_\omega &= -\|\tilde{b}_\omega\|^2 + \tilde{b}_\omega^\top \hat{R}^\top (I - \mathbf{E}(\tilde{R})) \hat{R} \tilde{b}_\omega \\ &\leq -\|\tilde{b}_\omega\|^2 + 2c_b^2 |\tilde{R}|_I^2. \end{aligned}$$

Moreover, in view of (A.14), the following upper bound for σ_2 can be derived

$$\|\sigma_2\| \leq 4\lambda_{\max}^{\mathbf{E}(M)} |\tilde{R}|_I + \rho_2 c_2 \gamma \|\zeta\|. \quad (\text{A.17})$$

It follows, using (Berkane, 2017, (18)), that

$$\begin{aligned} -k_1 \tilde{b}_\omega^\top \hat{R}^\top \mathbf{E}(\tilde{R}) \hat{R} \sigma_2 &= k_1 \tilde{b}_\omega^\top \hat{R}^\top (I - \mathbf{E}(\tilde{R})) \hat{R} \sigma_2 - \\ k_1 \tilde{b}_\omega^\top \sigma_2 &\leq k_1 |\tilde{R}|_I^2 \tilde{b}_\omega^\top \sigma_2 + k_1 \sqrt{2} |\tilde{R}|_I \|\tilde{b}_\omega\| \|\sigma_2\| - \\ k_1 \tilde{b}_\omega^\top \sigma_2 &\leq -k_1 \tilde{b}_\omega^\top \sigma_2 + 8k_1 \lambda_{\max}^{\mathbf{E}(M)} c_b (\sqrt{2} + 2) |\tilde{R}|_I^2 + \\ &\quad 2k_1 \gamma \rho_2 c_b c_2 (\sqrt{2} + 2) |\tilde{R}|_I \|\zeta\|. \end{aligned}$$

Besides, the following bounds are easily derived

$$\begin{aligned} &-\tilde{b}_\omega^\top [\omega + \tilde{b}_\omega + k_1 \sigma_2] \times \hat{R}^\top \psi(\tilde{R}) \\ &= -\tilde{b}_\omega^\top [\omega + k_1 \sigma_2] \times \hat{R}^\top \psi(\tilde{R}) \\ &\leq c_\omega \|\tilde{b}_\omega\| \|\psi(\tilde{R})\| + k_1 \|\tilde{b}_\omega\| \|\psi(\tilde{R})\| \|\sigma_2\| \\ &\leq 2c_\omega \|\tilde{b}_\omega\| |\tilde{R}|_I + 16k_1 \lambda_{\max}^{\mathbf{E}(M)} c_b |\tilde{R}|_I^2 + \\ &\quad + 4k_1 \gamma \rho_2 c_b c_2 |\tilde{R}|_I \|\zeta\|. \end{aligned}$$

and

$$\begin{aligned} \mathbf{P}_{c_s}^{\epsilon_b} (\hat{b}_\omega, k_2 \sigma_2)^\top \hat{R}^\top \psi(\tilde{R}) &\leq k_2 \|\sigma_2\| \|\psi(\tilde{R})\| \\ &\leq 4k_2 \lambda_{\max}^{\mathbf{E}(M)} |\tilde{R}|_I^2 + 2k_2 \gamma \rho_2 c_2 |\tilde{R}|_I \|\zeta\|. \end{aligned}$$

Consequently, one deduces that

$$\begin{aligned} \dot{\hat{\mathbf{x}}} &\leq -\|\tilde{b}_\omega\|^2 - k_1 \tilde{b}_\omega^\top \sigma_2 + (\alpha_1 + k_1 \alpha_2) |\tilde{R}|_I^2 + \\ &\quad \gamma (\alpha_3 + k_1 \alpha_4) |\tilde{R}|_I \|\zeta\| + 2c_\omega \|\tilde{b}_\omega\| |\tilde{R}|_I, \quad (\text{A.18}) \end{aligned}$$

where $\alpha_1 = 8c_b^2 + 4k_2 \lambda_{\max}^{\mathbf{E}(M)}$, $\alpha_2 = 8\lambda_{\max}^{\mathbf{E}(M)} c_b (\sqrt{2} + 4)$, $\alpha_3 = 2k_2 \rho_2 c_2$ and $\alpha_4 = 2\rho_2 c_b c_2 (\sqrt{2} + 4)$. Consequently, in view of the above obtained results, one has

$$\begin{aligned} \dot{\mathbf{W}} &\leq -4k_1 \lambda_{\min}^{\mathbf{E}(M)} (1 - \epsilon^2) |\tilde{R}|_I^2 - \mu_1 \|\tilde{b}_\omega\|^2 \\ &\quad + 2\gamma c_2 \beta_2 \|\zeta\| \|\tilde{b}_\omega\| + (1 + 2\mu_1 c_\omega) |\tilde{R}|_I \|\tilde{b}_\omega\| \\ &\quad + \mu_1 (\alpha_1 + k_1 \alpha_2) |\tilde{R}|_I^2 - \gamma^3 \|\zeta\|^2 \\ &\quad + \gamma (k_1 \rho_2 c_2 + 4\sqrt{2} \beta_2 c_3 + \mu_1 (\alpha_3 + k_1 \alpha_4)) |\tilde{R}|_I \|\zeta\| \\ &= -\varsigma_{12}^\top P_{12} \varsigma_{12} - \varsigma_{13}^\top P_{13} \varsigma_{13} - \varsigma_{23}^\top P_{23} \varsigma_{23} \end{aligned} \quad (\text{A.19})$$

where $\varsigma_{ij} = [\varsigma_i, \varsigma_j]^\top$ and the matrices P_{ij} are given by

$$\begin{aligned} P_{12} &= \begin{bmatrix} k_1 (2\lambda_{\min}^{\mathbf{E}(M)} (1 - \epsilon^2) - \mu_1 \alpha_2) - \mu_1 \alpha_1 & -(\frac{1}{2} + c_\omega \mu_1) \\ * & \frac{\mu_1}{2} \end{bmatrix} \\ P_{13} &= \begin{bmatrix} 2k_1 \lambda_{\min}^{\mathbf{E}(M)} (1 - \epsilon^2) & -\frac{\gamma}{2} (k_1 \rho_2 c_2 + 4\sqrt{2} \beta_2 c_3 + \\ & + \mu_1 (\alpha_3 + k_1 \alpha_4)) \\ * & \frac{\gamma^3}{2} \end{bmatrix} \\ P_{23} &= \begin{bmatrix} \frac{\mu_1}{2} & -\gamma \beta_2 c_2 \\ -\gamma \beta_2 c_2 & \frac{\gamma^3}{2} \end{bmatrix}. \end{aligned}$$

Now, if we pick $\mu_1 > 0$ such that $\mu_1 < \lambda_{\min}^{\mathbf{E}(M)} (1 - \epsilon^2) / \alpha_2$ and choose the gains k_1 and γ such that

$$\begin{aligned} k_1 &> \max \left\{ 2\mu_1 k_2, \frac{2\alpha_1 \mu_1^2 + (1 + 2c_\omega \mu_1)^2}{2\mu_1 \lambda_{\min}^{\mathbf{E}(M)} (1 - \epsilon^2)} \right\}, \\ \gamma &> \max \left\{ \frac{4(\beta_2)^2 c_2^2}{\mu_1}, \right. \\ &\quad \left. \frac{(k_1 \rho_2 c_2 + 4\sqrt{2} \beta_2 c_3 + \mu_1 (\alpha_3 + k_1 \alpha_4))^2}{4k_1 \lambda_{\min}^{\mathbf{E}(M)} (1 - \epsilon^2)} \right\}, \end{aligned}$$

then we can verify that matrices P_1, P_2, P_{12}, P_{13} and P_{23} are all positive definite. The exponential stability immediately follows.

References

- Batista, P., Silvestre, C., and Oliveira, P. (2011). Single range aided navigation and source localization: Observability and filter design. *Systems and Control Letters*, 60(8):665–673.
- Batista, P., Silvestre, C., and Oliveira, P. (2016). Tightly coupled long baseline/ultra-short baseline integrated navigation system. *International Journal of Systems Science*, 47(8):18371855.
- Berkane, S. (2017). Attitude Estimation with Intermittent Measurements. *Automatica*.
- Berkane, S., Abdessameud, A., and Tayebi, A. (2017). Hybrid Attitude and Gyro-bias Observer Design on SO(3). *IEEE Transactions on Automatic Control*, 62(11):6044–6050.
- Berkane, S. and Tayebi, A. (2017a). Attitude and Gyro Bias Estimation Using GPS and IMU Measurements. In *IEEE 56th Conference on Decision and Control*, pages 2402–2407.
- Berkane, S. and Tayebi, A. (2017b). Construction of Synergistic Potential Functions on SO(3) with Application to Velocity-Free Hybrid Attitude Stabilization. *IEEE Transactions on Automatic Control*, 62(1):495–501.
- Berkane, S. and Tayebi, A. (2017c). On the Design of Attitude Complementary Filters on SO(3). *IEEE Transactions on Automatic Control*, 63(3):880–887.
- Berkane, S. and Tayebi, A. (2019). Position, velocity, attitude and gyro-bias estimation from imu and position information. In *18th European Control Conference (ECC)*, pages 4028–4033.
- Bryne, T. H., Hansen, J. M., Rogne, R. H., Sokolova, N., Fossen, T. I., and Johansen, T. A. (2017). Nonlinear Observers for Integrated Implementation Aspects. *IEEE Control Systems Magazine*, 37(3):59–86.
- Bucy, R. S. (1967). Global theory of the Riccati equation. *Journal of Computer and System Sciences*, 1(4):349–361.
- Bucy, R. S. (1972). The riccati equation and its bounds. *Journal of Computer and System Sciences*, 6(4):343–353.

- Crassidis, J. L. (2006). Sigma-point Kalman filtering for integrated GPS and inertial navigation. *IEEE Transactions on Aerospace and Electronic Systems*, 42(2):750–756.
- Farrell, J. (2008). *Aided navigation: GPS with high rate sensors*. McGraw-Hill, Inc.
- Grip, H. F., Fossen, T. I., Johansen, T. A., and Saberi, A. (2013). Nonlinear Observer for GNSS-Aided Inertial Navigation with Quaternion-Based Attitude Estimation. In *American Control Conference*, pages 272–279.
- Gryte, K., Hansen, J. M., Johansen, A., and Fossen, T. I. (2017). Robust Navigation of UAV using Inertial Sensors Aided by UWB and RTK GPS. *AIAA Guidance, Navigation, and Control Conference*, (January).
- Hamel, T. and Samson, C. (2017). Position estimation from direction or range measurements. *Automatica*, 82:137–144.
- Hamel, T. and Samson, C. (2018). Riccati Observers for the Nonstationary PnP Problem. *IEEE Transactions on Automatic Control*, 63(3):726–741.
- Hamer, M. and D’Andrea, R. (2018). Self-calibrating ultra-wideband network supporting multi-robot localization. *IEEE Access*, 6:22292–22304.
- Hua, M.-d. (2010). Attitude estimation for accelerated vehicles using GPS/INS measurements. *Control Engineering Practice*, 18(7):723–732.
- Johansen, T. A. and Fossen, T. I. (2016). Nonlinear Observer for Tightly Coupled Integration of Pseudorange and Inertial Measurements. *IEEE Transactions on Control Systems Technology*, 24(6):2199–2206.
- Johansen, T. A., Hansen, J. M., and Fossen, T. I. (2016). Nonlinear Observer for Tightly Integrated Inertial Navigation Aided by Pseudo-Range Measurements. *Journal of Dynamic Systems, Measurement, and Control*, 139(1):011007.
- Johansen, T. A., Hansen, J. M., and Fossen, T. I. (2018). Nonlinear Observer for Tightly Coupled Integrated Inertial Navigation Aided by RTK-GNSS Measurements. *IEEE Transactions on Control Systems Technology*, to appear, pages 1–16.
- Kai, J.-M., Allibert, G., Hua, M.-D., and Hamel, T. (2017). Nonlinear feedback control of quadrotors exploiting first-order drag effects. *IFAC-PapersOnLine*, 50(1):8189 – 8195. 20th IFAC World Congress.
- Krstic, M., Kanellakopoulos, I., and Kokotovic, P. V. (1995). *Nonlinear and adaptive control design*. Wiley New York.
- Mahony, R., Hamel, T., and Pfimlin, J.-m. (2008). Nonlinear Complementary Filters on the Special Orthogonal Group. *IEEE Transactions on Automatic Control*, 53(5):1203–1218.
- Titterton, D., Weston, J. L., and Weston, J. (2004). *Strapdown inertial navigation technology*, volume 17. IET.
- Vasconcelos, J. F., Silvestre, C., and Oliveira, P. (2008). A nonlinear gps/imu based observer for rigid body attitude and position estimation. In *2008 47th IEEE Conference on Decision and Control*, pages 1255–1260. IEEE.
- Wang, B.-Y. and Zhang, F. (1994). A trace inequality for unitary matrices. *The American Mathematical Monthly*, 101(5):453–455.
- Whittaker, M. and Crassidis, J. L. (2017). Inertial Navigation Employing Common Frame Error Representations. *AIAA Guidance, Navigation, and Control Conference*, pages 1–24.
- Woodman, O. J. (2007). An introduction to inertial navigation. *Technical Report, University of Cambridge Computer, Laboratory*, (UCAM-CL-TR-696):1–37.
- Zlotnik, D. E., Member, S., and Forbes, J. R. (2016). Nonlinear Estimator Design on the Special Orthogonal Group using Vector Measurements Directly. *IEEE Transactions on Automatic Control*, 9286(c):1–12.